Neurobiology of Stress 13 (2020) 100226

Contents lists available at ScienceDirect

Neurobiology of Stress

journal homepage: www.elsevier.com/locate/ynstr

Brain-wide mapping of c-fos expression in the single prolonged stress model and the effects of pretreatment with ACH-000029 or prazosin

Hatylas Azevedo[a,*,1], Marcos Ferreira[a,1], Alessandra Mascarello[a], Pavel Osten[b,c], Cristiano Ruch Werneck Guimarães[a]

[a] Aché Laboratórios Farmacêuticos, Guarulhos, São Paulo, Brazil
[b] Cold Spring Harbor Laboratories, Cold Spring Harbor, NY, USA
[c] Certerra Inc., Cold Spring Harbor, NY, USA

ARTICLE INFO

Keywords:
Single prolonged stress
C-fos
Brain regions
Post traumatic stress disorder
ACH-000029

ABSTRACT

Post-traumatic stress disorder (PTSD) is a mental health condition that is triggered by a stressful event, with symptoms including exaggerated startle response, intrusive traumatic memories and nightmares. The single prolonged stress (SPS) is a multimodal stress protocol that comprises a sequential exposure to physical restraint, forced swimming, predator scent and ether anesthesia. This procedure generates behavioral and neurobiological alterations that resemble clinical findings of PTSD, and thus it is commonly used to model the disease in rodents. Here, we applied c-fos mapping to produce a comprehensive view of stress-activated brain regions in mice exposed to SPS alone or to SPS after oral pretreatment with the serotonin-noradrenaline receptor dual modulator ACH-000029 or the α1-adrenergic blocker prazosin. The SPS protocol evoked c-fos expression in several brain regions that control the stress-anxiety response, including the central and medial amygdala, the bed nucleus of the stria terminalis, the pallidum, the paraventricular hypothalamus, the intermediodorsal, paraventricular and central medial thalamic nuclei, the periaqueductal gray, the lateral habenula and the cuneiform nucleus. These effects were partially blocked by pretreatment with prazosin but completely prevented by ACH-000029. Collectively, these findings contribute to the brain-wide characterization of neural circuits involved in PTSD-related stress responses. Furthermore, the identification of brain areas regulated by ACH-000029 and prazosin revealed regions in which SPS-induced activation may depend on the combined or isolated action of the noradrenergic and serotonergic systems. Finally, the dual regulation of serotonin and α1 receptors by ACH-000029 might represent a potential pharmacotherapy that can be applied in the peri-trauma or early post-trauma period to mitigate the development of symptoms in PTSD patients.

1. Introduction

Post-traumatic stress disorder (PTSD) is a debilitating psychiatric condition defined by a persistent and amplified emotional response to past traumatic experiences. PTSD symptoms are comprised of intrusive thoughts, avoiding reminders, sleep disturbance and increased arousal (American Psychiatric Association, 2013). Although some patients benefit from the available pharmacotherapy, most experience only temporary and limited suppression of their symptoms after treatment (Bernardy and Friedman, 2015; Starke and Stein, 2017).

Animal models have been used to study the development of PTSD-like symptoms after a traumatic event (Flandreau and Toth, 2018). These models usually involve exposure of the animal to a severe, unpredictable, and inescapable stressor to avoid habituation and mimic the life-threatening trauma suffered by patients. Most models utilize physical and psychological stressors such as single prolonged stress (SPS), predator scent stress, immobilization stress, unpredictable variable stress and social defeat stress to mimic this condition (Borghans and Homberg, 2015; Deslauriers et al., 2018). Animals subjected to these models exhibit behavioral alterations such as anxiety-like or fear-related avoidance behavior and neurobiological changes, including glucocorticoid receptor (GR) hypersensitivity and amygdala hyperactivity (Aspesi and Pinna, 2019). The SPS protocol, for example, uses multiple stressors to induce a broad range of PTSD-related behavioral

* Corresponding author. Research, Development and Innovation, Aché Laboratórios Farmacêuticos, Rodovia Presidente Dutra km 222,2, Guarulhos, 07034-904, São Paulo, SP, Brazil.
E-mail address: hatylas.azevedo@ache.com.br (H. Azevedo).
[1] These authors contributed equally to this work.

https://doi.org/10.1016/j.ynstr.2020.100226
Received 15 January 2020; Received in revised form 12 March 2020; Accepted 1 May 2020
Available online 13 May 2020

and molecular changes (Liberzon et al., 1999; Perrine et al., 2016; Souza et al., 2017). Many phenotypes appear only after a 1-week period, offering a time window for the study of PTSD pathogenesis (Lisieski et al., 2018; Deslauriers et al., 2018).

Previous work using the above-described models has shown that molecular changes, including alterations in the serotonin (5-HT) and noradrenergic (NE) neurotransmitter systems (Krystal and Neumeister, 2009; Hendrickson and Raskind, 2016), are associated with PTSD. In the SPS model, 5-HT1A and 5-HT2A receptors, which regulate anxiety levels, show increased expression in the dorsal raphe nucleus and the hippocampus (Luo et al., 2011; Xiang et al., 2019). In addition, in this model, 5-HT1A activity is related to neuronal apoptosis of the amygdala (Liu et al., 2011) and to GR expression in the hypothalamus (Wang et al., 2009), and pretreatment with a 5-HT1A antagonist partially inhibits these alterations. Similarly, α1 and α2-adrenergic receptors play a role in the increased startle response, aggressive behavior, and social interaction deficits seen in fear conditioning (Olson et al., 2011), predator stress (Rajbhandari et al., 2015) and SPS (Toledano et al., 2013) models.

During our exploration of the interaction between the 5-HT and NE systems, we have discovered a novel compound, ACH-000029, that modulates the activity of specific 5-HT and α1-adrenergic receptors. This compound acts as a nanomolar potent partial agonist of 5-HT1A/D receptors and as an antagonist of 5-HT2A and α1-adrenergic receptors, and does not show any relevant activity on other 5-HT and noradrenergic receptors, as well as on GABAergic, glutamatergic, dopaminergic and histaminergic receptors (Azevedo et al., 2019). ACH-000029 was also shown to exhibit high blood-brain barrier permeation in mice and acute anxiolytic effects in oral doses ranging from 16 to 30 mg/kg (Azevedo et al., 2019). In addition, the 7-day treatment with ACH-000029 after the SPS procedure ameliorated the SPS-induced sociability impairment and anxiety-like behavior, and modulated c-fos changes in brain regions involved in anxiety response, like the globus pallidus, lateral septum, cerebellum, retrosplenial cortex and ventromedial hypothalamus (Azevedo et al., 2020).

In this study, we examined the brain-wide distribution of c-fos in mice pretreated with vehicle, ACH-000029 or prazosin, and subjected to the SPS or Sham protocols. The analysis of immediate-early genes (IEGs) such as c-fos, Egr1 and arc as surrogate markers of neural activity is relevant to gain insights into psychiatric disorders and the action of drugs in the brain (Gallo et al., 2018). Thus, new studies assessing IEG expression patterns may help to unravel the molecular mechanisms by which drugs affect behavior in PTSD animal models (De Bartolomeis et al., 2017). The α1-adrenergic blocker prazosin was included as a comparator because it is used off-label to treat anxiety and nightmares in established PTSD (De Berardis et al., 2015; Khachatryan et al., 2016). Some authors have also discussed the potential of using prazosin and other drugs as prophylactic or early treatments in the prevention of PTSD by limiting the stress experience or interfering with the consolidation of the traumatic memory in patients who visit an emergency department after trauma (Green, 2014; Roque, 2015; Burbiel, 2015; Linares et al., 2017; ClinicalTrials.gov identifier NCT03045016). This could be also the case for patients diagnosed with acute stress disorder (ASD), which is characterized by acute stress reactions, like intrusion, dissociation, negative mood, avoidance, and arousal, that may occur in the initial month after a traumatic event (Bryant, 2018).

2. Materials and methods

2.1. Drugs

Prazosin was purchased from Sigma-Aldrich (St. Louis, MO, USA), and ACH-000029 was synthesized at Aché Laboratórios (Guarulhos, SP, Brazil). The compounds were dissolved in distilled water containing 0.2% hydroxypropyl methylcellulose (vehicle). The doses of ACH-000029 and prazosin used in this study were selected based on the previous literature (Azevedo et al., 2019, 2020; Knauber and Müller, 2000; Stone and Zhang, 1995). The drugs were administered per oral (p.o.) by gavage.

2.2. Animals

Male C57BL/6 mice (8–10 weeks of age) were obtained from the Cold Spring Harbor Laboratory (CSHL). The animals were housed in pairs at room temperature of 23 ± 2 °C, relative humidity of 60 ± 10% and artificial lighting between 7:00 and 19:00. Food and water were available *ad libitum*. The animals were maintained in accordance with the Animal Welfare Act and the Department of Health and Human Services Guide for the Care and Use of Laboratory Animals. CSHL's animal facility is accredited by the American Association for Accreditation of Laboratory Animal Care. The animal procedures used in this study were approved by the CSHL's ethics committee (number 933272-15).

2.3. Single prolonged stress protocol (SPS)

The SPS protocol was conducted as described in Perrine et al. (2016) and Malikowska et al. (2017). Each mouse was restrained for 1 h in a BD Falcon© 50-mL conical tube with a screw-on top and air holes located 1/2 cm apart; following the restraint, the animals underwent a 20-min group swim session (n = 4–8 mice per swim) in a 4-L beaker (diameter = 18.4 cm) filled with water to a depth of ~25 cm (3.5 L) at room temperature (~23 °C). The animals were then towel dried and returned to their original cages, where they were exposed for 15 min to the predator cue using soiled bedding from the cages of sentinel rats. The mice were then exposed to increasing concentrations of diethyl ether until they lost consciousness. Diethyl ether-soaked cotton balls were added at 1-min intervals to minimize the rapid onset of loss of consciousness. Sham animals were handled and allowed to explore an empty 4-L beaker for a period equivalent to the duration of the protocol. Previous studies have shown that increased c-fos expression is observed for at least 2–3 h after the novel context exposure (VanElzakker et al., 2008; Bisler et al., 2002). At the end of the protocol, the animals were placed in new cages with fresh bedding and returned to the vivarium.

2.4. Experimental protocol and groups

Mice (n = 10 per group) were randomized into (i) Vehicle-Sham, (ii) Vehicle-SPS, (iii) ACH-000029-SPS and (iv) Prazosin-SPS groups. The animals were pretreated with vehicle, ACH-000029 (30 mg/kg p.o.) or prazosin (10 mg/kg p.o.) 30 min before the SPS or Sham protocol was initiated. Brain c-fos expression was analyzed 60 min after the end of the SPS protocol and was performed blind to the treatment groups. The c-fos expression was assessed at this timepoint to capture c-fos induction derived from all steps of the stress procedure, which is in line with other studies that analyzed c-fos expression 60 min after the stress period (Lin et al., 2018; Martinez et al., 2002; Hoffman et al., 1993). The animals were anesthetized with ketamine/xylazine and sacrificed by transcardial perfusion with saline and 4% formaldehyde, and their brains were dissected and post-fixed.

2.5. Brain-wide c-fos expression analysis

Neuronal activation in the mouse brain was mapped at single-cell resolution using the same brain-wide c-fos immunohistochemistry procedure described elsewhere (Osten and Margrie, 2013; Renier et al., 2016), which evaluates more than 800 anatomical regions of interest (ROIs) from the Allen Mouse Brain Atlas. Samples were imaged in sagittal orientation (right lateral side up) using light-sheet fluorescence microscopy (Ultramicroscope II, LaVision Biotec, Bielefeld, Germany).

The c-fos positive (c-fos+) neurons were identified by convolutional neural networks and visualized in 3D, as described in Kim et al. (2015). The CN configuration included 3 hidden layers. The data set was divided into 6 folds and five CNs were trained with each training set. Of the five CNs, the CN with maximum F-score on its test data was selected. The CN training was performed using the Cortical network simulator (Mutch et al., 2010). The datasets were warped in 3D by affine and B-spline transformation to an average reference mouse brain generated from the brains of forty 8-week-old C57BL/6 mice (Kim et al., 2015, 2016). The data are reported as bar graph representations or anatomical visualizations in which neuronal activation is represented by an increase in c-fos+ cells and visualized as a "red" signal. Analogously, neuronal inhibition is represented by a decrease in c-fos + cells and is visualized as a "green" signal overlaid on a grayscale image of the mouse brain. Selected ROIs were drawn as dashed white lines in the images.

2.6. Statistical data analysis

Statistical comparisons between the groups were made based on the ROIs as described in details elsewhere (Kim et al., 2015, 2016). The cell counts at a given location, Y, were assumed to follow a negative binomial distribution the mean of which is linearly related to one or more of the experimental conditions, X: $E[Y] = \alpha + \beta X$. For example, when comparing an experimental group with a control group, X is a single column showing the categorical classification of the sample according to its group id, i.e., 0 for the control group and 1 for the experimental group. The maximum likelihood coefficients α and β were found through an iterative reweighted least squares method, obtaining estimates for sample standard deviations and estimates of significance for the β coefficient. A significant β indicates that the group status is related to the cell count intensity at the specified location. Z-values were calculated based on the β coefficient normalized by its standard deviation, which under the null hypothesis of no group effect has an asymptotic standard normal distribution. The p-value is the probability of finding a β coefficient as extreme as the one seen by chance if the null hypothesis is true. To account for multiple comparisons across all ROI locations, the p-values were thresholded at a false discovery rate (FDR) of 5% (q-value) using the Benjamini-Hochberg (BH) procedure (Benjamini and Hochberg, 1995). The BH procedure compares each original (uncorrected) p-value to its critical value, (i/m) *Q, where i is the rank of the individual p-value in ascending order, m is the total number of tests, and Q is the FDR. The largest p-value with $p < (i/m) *Q$ is considered to be the significance threshold. Scatter plots were also built to compare the z-scores of each brain region between the SPS-vehicle versus Sham-vehicle comparison (x-axis) and the ACH-000029 or prazosin-treated groups (y-axis). The graph elements represent the brain regions and were illustrated with green or red colors when z-scores were less than −2 (downregulated) or larger than +2 (upregulated), respectively.

3. Results and discussion

3.1. Brain-wide c-fos mapping of regions activated and deactivated by the SPS protocol

The comparative analysis of c-fos expression in the brains of animals from the Vehicle-SPS and Vehicle-Sham groups disclosed regions that are regulated by the SPS procedure. Table S1 lists all brain regions that showed differences in c-fos expression between the Vehicle-SPS and Vehicle-Sham groups. In Fig. 1, the differences in c-fos + cell counts between these groups are also shown for selected brain regions in the cerebral cortex, bed nucleus of the stria terminalis (BST), amygdala, thalamus, hypothalamus, hindbrain and midbrain. There was a large increase of c-fos+ cells in stress-related brain areas in the SPS group, such as in the prefrontal cortex, nucleus accumbens (ACB), BST, central amygdala (CEA), medial amygdala (MEA), midline thalamic nuclei, hypothalamic nuclei, brainstem and hindbrain - including the periaqueductal gray (PAG), parabrachial nucleus (PB), and raphe nuclei (Adhikari, 2014).

In the cerebral cortex (Fig. 1A and Table S1), brain activation (increased numbers of c-fos+ cells) and inactivation (decreased numbers of c-fos+ cells) were seen in various cortical areas in the Vehicle-SPS group. The most pronounced activation patterns were observed in the deep layers of the primary and secondary somatosensory cortex (SSp and SSs, respectively) and the posterior and ventral auditory cortex (AUDp and AUDv). Cortical inactivation across multiple cortical areas was also observed, with the most pronounced effect seen in the piriform cortex (PIR) and the olfactory tubercle (OT), the dorsal agranular insular cortex (AId), the ventral agranular insular cortex (AIv), the superficial layers of the SSp, and the superficial and middle layers of the primary visual cortex (VISp). Other areas in which inactivation was observed included the ventral and dorsal retrosplenial cortices (RSPv and RSPd), the ventrolateral area (ORBvl) and the ventral part of the anterior cingulate cortex (ACAv).

The cortical patterns seen in the Vehicle-SPS versus Vehicle-Sham comparison likely reflect the differences in the protocols to which these two groups were subjected. The first group was subjected to acute stress brought on by restraint, forced swimming, exposure to soiled bedding and ether anesthesia, while the second group was allowed to freely explore the novel context of a dry glass beaker and then placed in new clean cages. Thus, the inactivation patterns seen in the visual cortex, piriform cortex, and many associational areas of mice subjected to the SPS protocol - *i.e.* lower c-fos+ cell counts in the Vehicle-SPS *versus* the Vehicle-Sham group - may reflect either the different contextual experiences between these groups or the suppressive effect of SPS in these regions. In line with this conclusion, animals exposed to a single severe stressor or to chronic stress have c-fos levels lower than controls in some areas of the brain (Vallès et al., 2006; Knox et al., 2016; Moench et al., 2019), suggesting that enduring traumas could induce an adaptive response in the corticolimbic system.

The hippocampal formation (Fig. 1A and Table S1) primarily showed patterns of inactivation in the dorsal parts of the CA1, CA2 and CA3 fields, the dentate gyrus (DG) and the dorsal subiculum (SUBd), presubiculum (PRE) and postsubiculum (POST). Conversely, relatively minor activation was detected in the ventral subiculum (SUBv) and the adjacent medioventral entorhinal cortex (ENTmv). The predominant inactivation in the hippocampus, which was shown by the presence of more c-fos+ cells in the Sham group, likely reflects the above-mentioned exploration of the novel environment by these animals, as this type of spatially oriented activity is known to engage these brain structures.

In the dorsal part of the striatum, the caudoputamen (CP) did not show major differences in c-fos expression in the Vehicle-SPS and Vehicle-Sham groups. In the ventral part of the striatum, the ACB was activated rostrally in the SPS group. This field represented the ventral continuation of the c-fos activation in the caudal prelimbic (PL) and ILA (infralimbic) regions, neighboring the activation in the rostral part of the lateral septum (LSr), and continued caudally into a robust activation of essentially all BST nuclei (Fig. 1B, Table S1). Finally, both the central amygdala (CEA) and the medial amygdala (MEA) displayed robust c-fos activation in the SPS group. There was also a trend of increased c-fos expression in the basolateral (BLA, q-value = 0.060) and basomedial (BMA) amygdala (q = 0.078) in the SPS group. These patterns, especially in the ACB, BST, CEA and MEA, are consistent with the role of these structures in the brain stress-anxiety response and related psychiatric disorders (Lebow and Chen, 2016).

In the thalamus (Fig. 1C), the comparison of the Vehicle-SPS and the Vehicle-Sham groups revealed activation of the medial thalamic nuclei, including the medial group of the dorsal thalamus (MED), the intermediodorsal nucleus of the thalamus (IMD), the mediodorsal nucleus of the thalamus (MD), the submedial nucleus of the thalamus (SMT), the

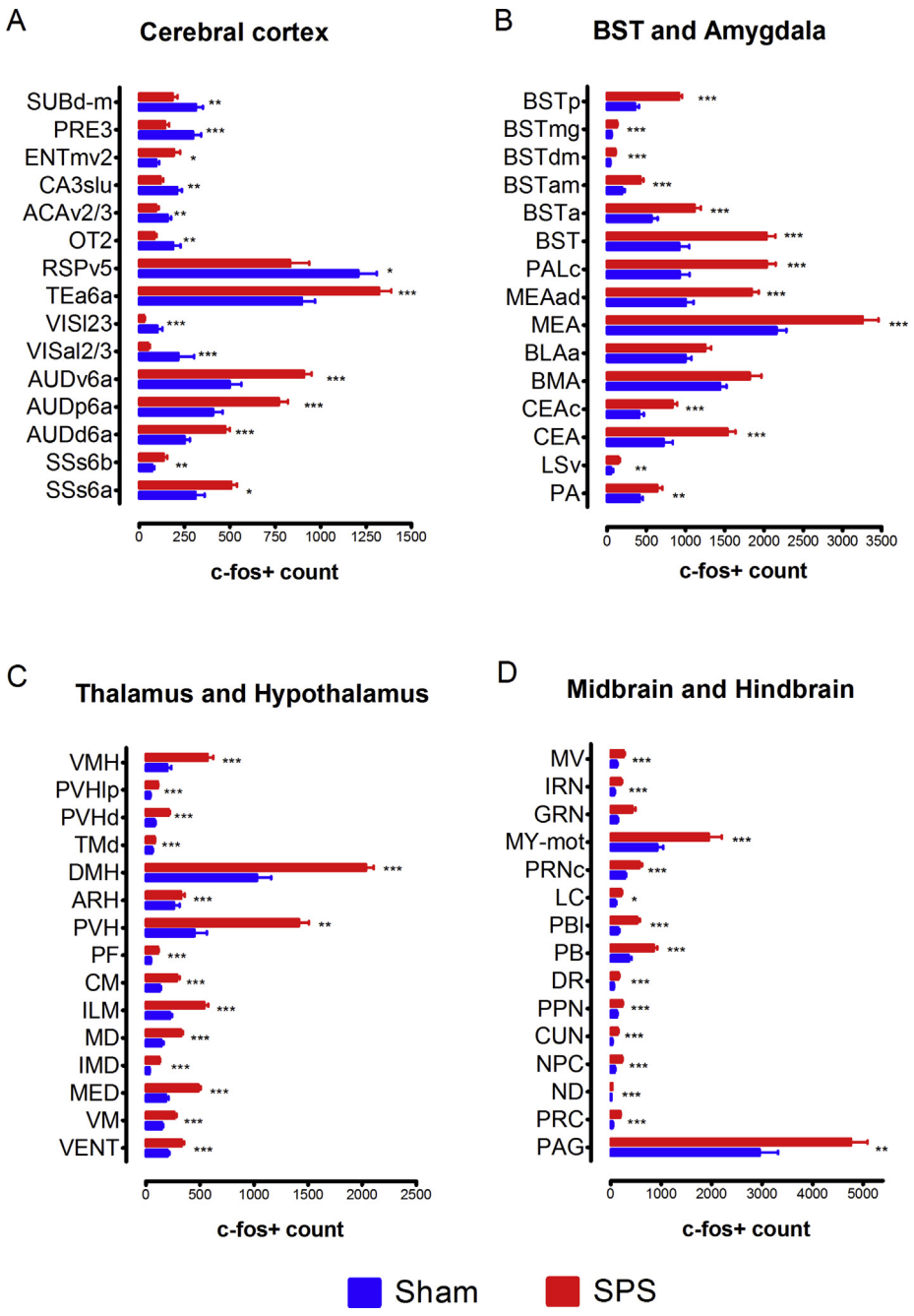

Fig. 1. Brain-wide c-fos mapping of regions regulated by the single prolonged stress (SPS) protocol in mice. Differences in c-fos+ cell counts between the Vehicle-SPS and Vehicle-Sham groups in selected regions of the cerebral cortex, the bed nucleus of the stria terminalis, the amygdala, the thalamus, the hypothalamus, the hindbrain and the midbrain are shown. *q < 0.05, **q < 0.01, ***q < 0.001. The c-fos expression was analyzed 60 min after the end of the SPS protocol.

midline group of the dorsal thalamus (MTN), including the paraventricular nucleus (PVT), and the intralaminar nuclei of the dorsal thalamus (ILM), including the rhomboid nucleus (RH), the central medial nucleus (CM), and the parafascicular nucleus (PF). These nuclei are part of the "limbic thalamus", which predominantly connects with limbic-related structures such as the amygdala and the nucleus accumbens and plays a role in affective behavior and drug-seeking activity (Vertes et al., 2015).

The SPS protocol induced a robust activation across the hypothalamus (Fig. 1C), which is a crucial area for the stress response mediated by the hypothalamo-pituitary-adrenal (HPA) system. The activated hypothalamic structures and the BST and CEA of the basal nuclei, which lie upstream to the hypothalamus in the stress response, connect densely with the paraventricular nucleus of the hypothalamus (PVH), which is an integrative structure of the HPA axis (Herman et al., 2016). The PVH also sends connections to midbrain and hindbrain nuclei that monitor changes in different systems of the body and provide upstream feedback; these nuclei were also activated by exposure of the animals to the SPS protocol.

The midbrain and hindbrain (Fig. 1D) also exhibited activation of stress-anxiety nodes. For example, the SPS protocol induced massive activation rostrocaudally in the PAG, most of the PB divisions, the central linear raphe nucleus (CLI), the dorsal raphe nucleus (DR) and in the locus coeruleus (LC). The activated region in the rostral PAG overlaps with the region that responds physiologically to stressors such as radiant heat and exposure to predators (Comoli et al., 2003). In

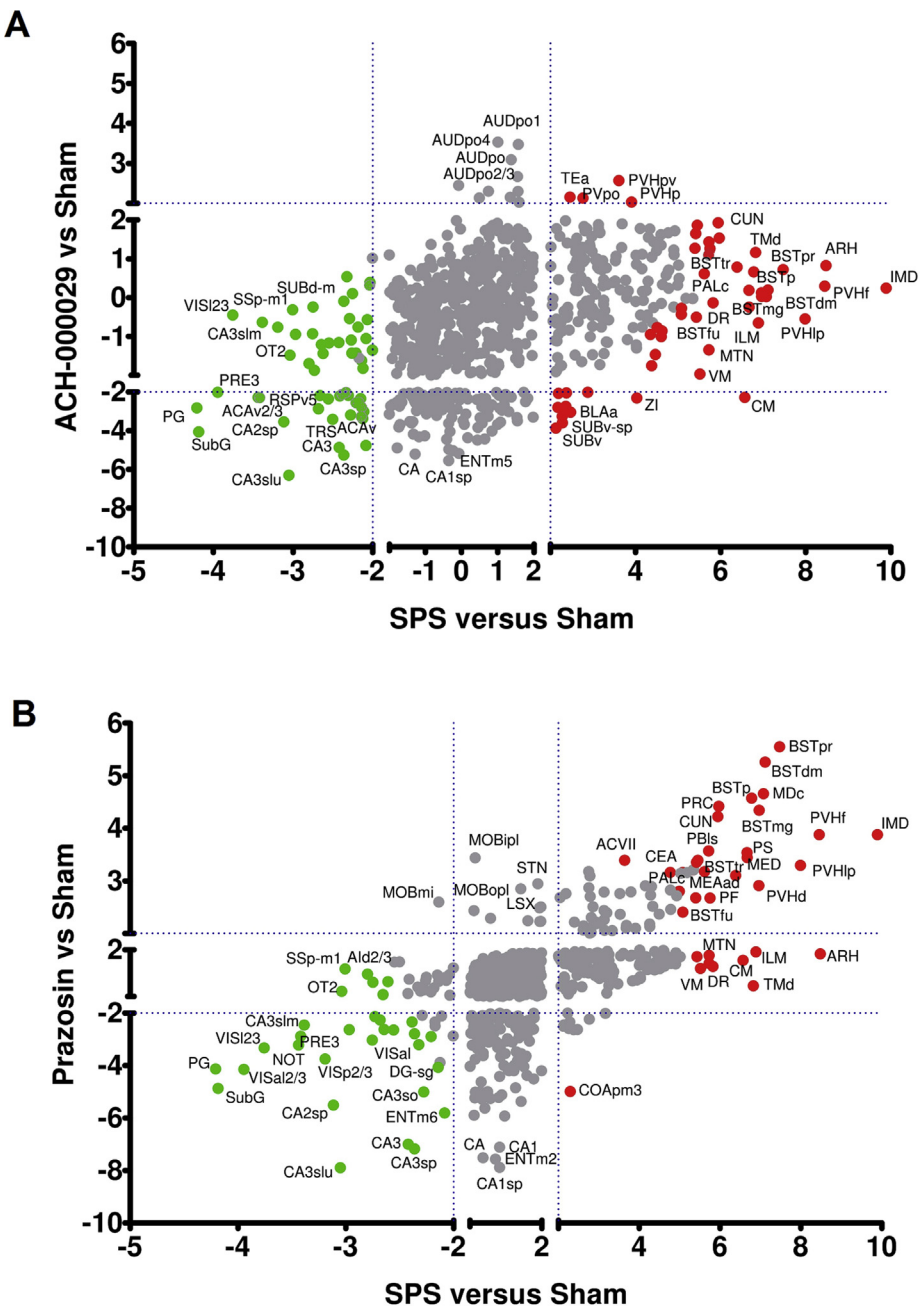

Fig. 2. Differential brain c-fos activation patterns for the comparisons between the drug-pretreated groups and the Vehicle-Sham group. (A) Scatter plot showing the relationship between the z-scores for each brain region in the comparisons Vehicle-SPS versus Vehicle-Sham (x-axis) and ACH-000029-SPS versus Vehicle-Sham (y-axis). (B) Scatter plot showing the relationship between the z-scores for each brain region in the comparisons Vehicle-SPS versus Vehicle-Sham (x-axis) and Prazosin-SPS versus Vehicle-Sham (y-axis). Brain regions that showed up- or downregulation of c-fos expression in the Vehicle-SPS group are represented as red and green circles, respectively. (For interpretation of the references to color in this figure legend, the reader is referred to the Web version of this article.)

parallel, the PB nuclei receive massive input from the hypothalamic nuclei and pain information from the dorsal horn of the spinal cord.

3.2. Brain areas with altered activity in the drug-pretreated and Vehicle-Sham groups

The comparisons between the ACH-000029-SPS and Vehicle-Sham groups and the Prazosin-SPS and Vehicle-Sham groups were performed to evaluate how far the brain activation patterns in mice pretreated with the test substances and subjected to the SPS protocol would be from a normal state in animals experiencing a novel context. The analysis was based on the following reasoning: i) if the drug pretreatment entirely mitigated the stress-induced response, the c-fos+ cell counts in the Sham and the drug-pretreated groups would be similar, and little difference would be observed in the comparisons; ii) if the drug had only a partial blocking effect, activation of stress-related structures would be observed in the drug-treated group, although to a lesser extent than in the Vehicle-SPS group.

Scatter plots were constructed to show the relationship between the z-scores for each brain area in the Vehicle-SPS versus Vehicle-Sham and ACH-000029-SPS (Fig. 2A) or Vehicle-SPS versus Vehicle-Sham and Prazosin-SPS (Fig. 2B) comparisons. Brain regions that were differentially regulated in the Vehicle-SPS group are displayed as red (up) or green (down) circles. Interestingly, almost no activation was found in the ACH-000029-SPS versus Vehicle-Sham comparison, whereas several stress-related structures were activated in the Prazosin-SPS group compared to the Vehicle-Sham group. This is illustrated by the much smaller number of brain structures seen in the upper-right quadrant of Fig. 2A compared to Fig. 2B.

In the cerebral cortex, the SPS protocol induced the activation of auditory and somatosensory areas, which was downregulated by pretreatment with either ACH-000029 or prazosin (Fig. 3A and B). A decrease in c-fos+ cells was seen in frontal cortical areas in both the ACH-000029-SPS and Prazosin-SPS groups, such as in the ILA and PL regions,

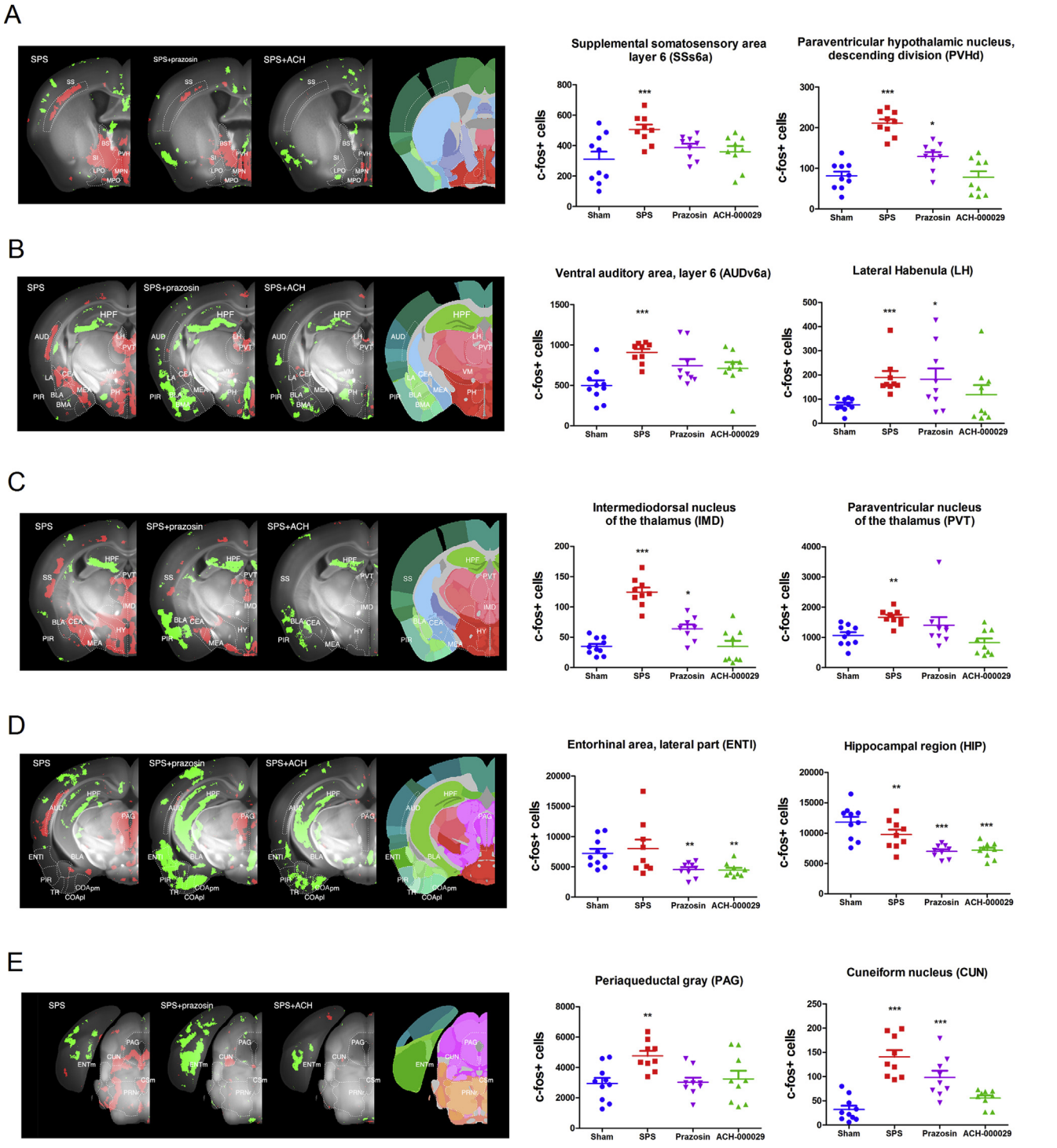

(caption on next page)

anterior cingulate cortex (ACC), piriform cortex, entorhinal area and cortical amygdala (Fig. 3B and D). Both the dorsal and the ventral hippocampus also showed inactivation in the groups pretreated with the test substances (Fig. 3D). This inactivation pattern in the hippocampus could be interpreted as a higher neuronal activity in the Sham group related to free exploration of a novel environment or to the suppressive effect of SPS in this region.

In the basal nuclei, no significant differences were observed in the ACH-000029-SPS versus Vehicle-Sham comparison. In contrast, the Prazosin-SPS versus Vehicle-Sham comparison revealed significant activation in the CP, ACB, BST, CEA, and MEA as well as in the lateral septum (Fig. 3A and B); higher c-fos+ cell counts were observed in these stress-related structures, showing that prazosin had only a partial counteracting effect.

In the hypothalamus, ACH-000029 also prevented the stress-evoked response; there was no significant difference in the number of c-fos + cells in the ACH-000029-SPS and Vehicle-Sham groups. In contrast, the number of c-fos+ cells was increased in the hypothalamus of mice from the Prazosin-SPS group. An example of the partial blocking effect of prazosin was also seen in the paraventricular hypothalamic nucleus (Fig. 3A), including the parvicellular neurons that project to the periaqueductal gray and to the parabrachial nucleus; this nucleus is the

Fig. 3. Anatomical description of brain regions regulated in the Vehicle-SPS and drug-pretreated groups compared to the Vehicle-Sham group. The data are reported as bar graph representations (mean + S.E.M.) or anatomical visualizations in which neuronal activation (increase in c-fos+ cell counts) or inhibition (decrease in c-fos+ cell counts) are visualized, respectively, as red or green signals overlaid on a grayscale image of a mouse brain. (A) SPS induced activation in the BST, PVH and MPN as well as in the deep layers of the somatosensory cortex (panel SPS). Pretreatment with prazosin only partially reduced the stress-induced activation in these structures (panel SPS + Prazosin), while the activation was nearly entirely abolished by pretreatment with ACH-000029 (panel SPS + ACH). (B) Prominent activation evoked by the SPS protocol is seen in the CEA, MEA, LA, PH, PVT, LH, and the deep layers of the AUD (panel SPS). Pretreatment with prazosin partially reduced the activation in the LH, CEA and PVT, while the activation was almost fully abolished by pretreatment with ACH-000029. Inhibition in the PIR, BLA and BMA was more pronounced after prazosin pretreatment. (C) SPS induced activation in the CEA, MEA, and HY (hypothalamus), the PVT (paraventricular nucleus of the thalamus) and the IMD (intermediodorsal nucleus of the thalamus) as well as in the SS. Prazosin partially reduced and ACH-000029 entirely abolished the stress-induced activation in these structures. (D) SPS-induced activation is seen in the PAG and deep layers of the AUD (panel SPS). Prazosin pretreatment partially reduced the stress-induced activation in PAG and AUD, while ACH-000029 completely abrogated this activation. Inhibition in the HPF was seen in all comparisons, while inhibition in the PIR, ENTl, and COA was more intense in mice pretreated with prazosin than in mice pretreated with ACH-000029. (E) Brainstem activation evoked by the SPS protocol is seen in the PAG and the CUN (cuneiform nucleus). CUN activation was partially reduced by prazosin but nearly entirely abolished by ACH-000029 pretreatment. ENTm inhibition was prominent in mice treated with prazosin. *q < 0.05, **q < 0.01, ***q < 0.001. Statistical comparisons were made against the Sham-Vehicle group. (For interpretation of the references to color in this figure legend, the reader is referred to the Web version of this article.)

primary driver of HPA responses (Herman and Tasker, 2016).

Likewise, no differences were seen in the thalamic nuclei in the Sham versus ACH-000029-SPS comparison, although several thalamic subnuclei were activated in the Prazosin-SPS group, including the medial, mediodorsal and intermediodorsal thalamic nuclei (Fig. 3C); this also indicates a partial blocking effect of prazosin. Another structure that showed a limited blocking effect of prazosin and a more suppressive effect of ACH-000029 was the lateral habenula (LH) in the epithalamus (Fig. 3B), a structure devoted to mood regulation and aversive encoding through modulation of the dopamine and serotonin systems (Lazaridis et al., 2019).

In the midbrain and hindbrain (Fig. 3E), a similar pattern was seen in stress-related structures such as the PAG, where there was no difference between the ACH-000029-SPS and Vehicle-Sham groups but a statistically significant activation in the Prazosin-SPS versus Vehicle-Sham comparison. This activation was, however, lower than that observed in the Vehicle-SPS versus Vehicle-Sham comparison (Fig. 3B). Another example is the cuneiform nucleus (Fig. 3C and D), a reticular nucleus involved in cardiovascular function and stress (Korte et al., 1992).

3.3. Brain areas with altered activity in the drug-pretreated and Vehicle-SPS groups

To further investigate whether the pretreatment with ACH-000029 or prazosin would limit the stress experience and the resulting brain activation evoked by the SPS protocol, we compared the Vehicle-SPS group with the ACH-000029-SPS group and with the Prazosin-SPS group. If the pretreatment with ACH-000029 or prazosin reduced the SPS-evoked stress response, this would be manifested as a relative inhibition of c-fos expression in the animals pretreated with these drugs. Accordingly, a very broad pattern of inhibition (significantly lower c-fos+ cell counts) was seen in stress-responsive brain structures in both the ACH-000029-SPS versus Vehicle-SPS comparison and in the Prazosin-SPS versus Vehicle-SPS comparison.

Fig. 4A and B show scatter plots indicating the up- and downregulated brain regions observed in the comparisons between the drug-pretreated groups and the Vehicle-SPS group (y-axis) compared to those observed in the Vehicle-SPS versus Vehicle-Sham (x-axis) comparison. Brain areas that were upregulated in the Vehicle-SPS versus Vehicle-Sham animals but downregulated in terms of c-fos+ cell counts in the comparisons between the drug-pretreated groups and the Vehicle-SPS group are shown as green circles. Brain regions that were downregulated in the Vehicle-SPS versus Vehicle-Sham groups but upregulated in the drug-pretreated groups are displayed as red circles.

ACH-000029 and prazosin mitigated SPS-induced c-fos activation in several stress-related brain regions, including the bed nucleus of the stria terminalis (BSTp, BSTpr, BSTtr, BSTmg, and BSTdm), the paraventricular hypothalamic nucleus (PVHd, PVHlp, and PVHf) and the ventral medial nucleus of the thalamus (VM). Only ACH-000029 downregulated c-fos+ cell counts in the intermediodorsal (IMD) and medial groups (MED) of nuclei in the dorsal thalamus and in the tuberomammillary nucleus (TMd). Neither of the drugs prevented c-fos activation in the arcuate hypothalamic nucleus (ARH) or in the epithalamus (EPI).

The representative brain images shown in Fig. 5A and B show that the cortical activation in the Vehicle-SPS group (shown in Fig. 3), including the activation in the SSp, SSs, AUDp and AUDv areas, was converted to inactivation by the pretreatment of the animals with either ACH-000029 or prazosin. Interestingly, the superficial and middle layers of the primary visual cortex (VISp) were activated in the ACH-000029-SPS group but not in the Prazosin-SPS group (Fig. 5B), suggesting higher activity in the visual cortex of the ACH-000029-pretreated mice. This indicates that the SPS protocol could induce a blunting effect in cortical sensory areas and ACH-000029-treated animals would exhibit activation in the visual cortex due to the attenuation of this stress response. In fact, habituation to repeated restraint stress was associated with lack of stress-induced c-fos expression in primary sensory processing areas (Girotti et al., 2006).

Fewer c-fos+ cells were also detected in the temporal association and cortical amygdalar areas in the mice pre-treated with the test substances (Fig. 5B). In the hippocampus, significant differences in c-fos activation between the Vehicle-SPS group and the drug-pretreated groups were observed in the dorsal hippocampus (Fig. 5B), while the ventral hippocampus appeared comparably inhibited in the ACH-000029 and prazosin groups. Because the dorsal hippocampus primarily performs cognitive functions whereas the ventral hippocampus relates to stress and affective behavior, the results suggest little difference in the cognitive experiences between the groups (Fanselow and Dong, 2010).

In the basal nuclei, the modest activation in the rostral CP seen in the SPS versus Sham comparison was converted into modest inactivation after administration of either drug, suggesting that this activation is specific to stress and that it is mitigated by both compounds. In contrast, only partial blocking of the stress response by prazosin was observed in the BST, CEA and MEA, whereas the deactivation in these areas was very pronounced in the ACH-000029-SPS group (Fig. 5A and D).

In the thalamus (Fig. 5C), the activation of the medial thalamic nuclei seen in the Vehicle-SPS group was converted to patterns of inactivation in the Vehicle-SPS versus ACH-000029-SPS and Vehicle-SPS versus Prazosin-SPS comparisons, with a more pronounced inhibitory effect in the ACH-000029-treated group. Similarly, the activation across the entire hypothalamus (Fig. 5C) was mitigated by both ACH-000029 and prazosin; in some regions of the hypothalamus, including the medial preoptic area (MPO) and the PVT (Fig. 5A), the decrease in the number of c-fos+ cells was more pronounced with ACH-000029 pretreatment. In the stress-related structures in the midbrain and

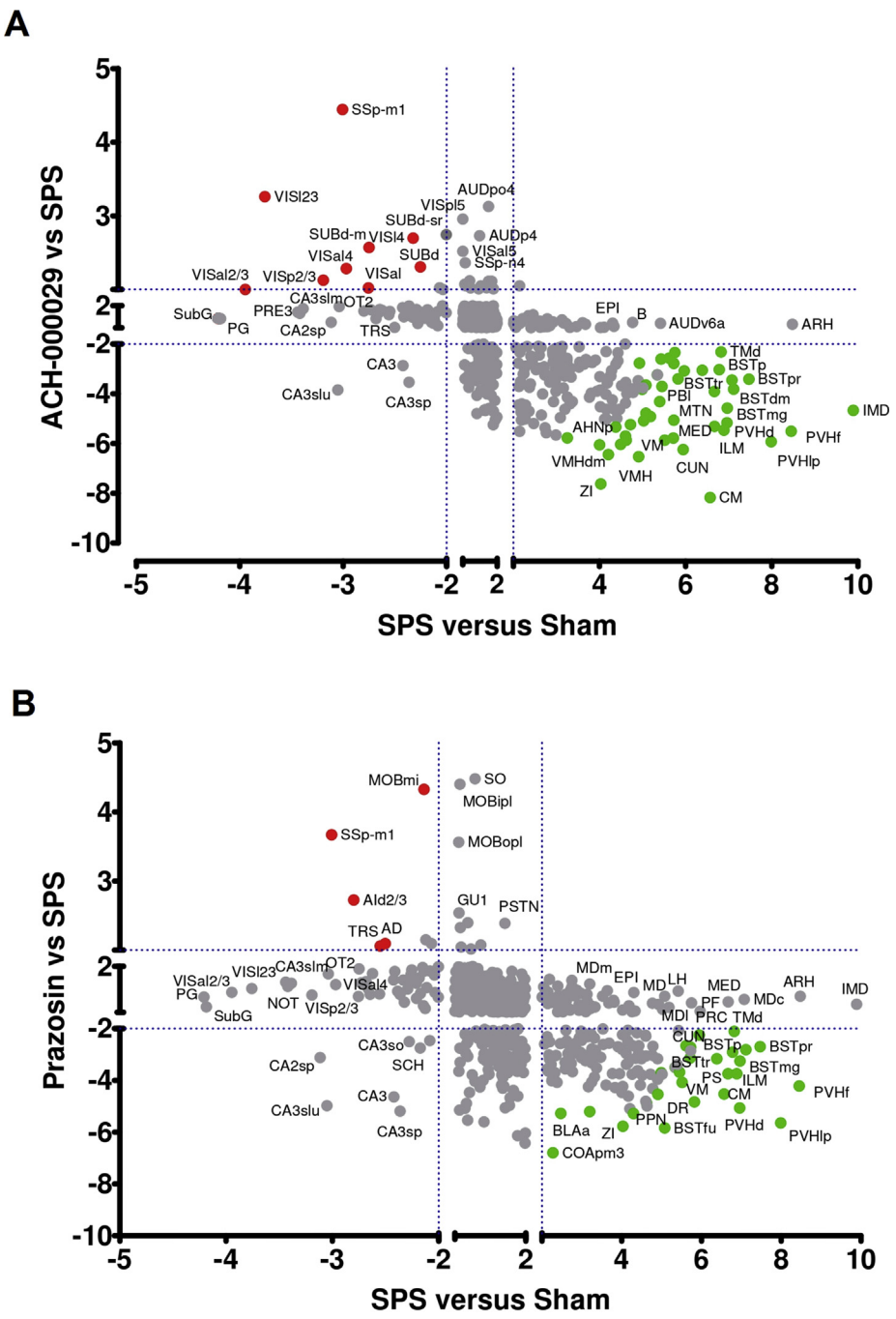

Fig. 4. Differential brain c-fos activation pattern obtained through comparisons between the drug-pretreated groups and the Vehicle-SPS group. (A) Scatter plot showing the relationship between the z-scores for each brain region in the Vehicle-SPS versus Vehicle-Sham (x-axis) and ACH-000029-SPS versus Vehicle-SPS (y-axis) comparisons. (B) Scatter plot showing the relationship between the z-scores for each brain region in the Vehicle-SPS versus Vehicle-Sham (x-axis) and Prazosin-SPS versus Vehicle-SPS (y-axis) comparisons. Brain areas upregulated in the Vehicle-SPS group but downregulated in the drug-pretreated groups are represented as green circles. Regions downregulated in the Vehicle-SPS but upregulated in the drug-pretreated groups are displayed as red circles. (For interpretation of the references to color in this figure legend, the reader is referred to the Web version of this article.)

hindbrain, a similar inhibitory effect was also seen in the groups that were pretreated with the tested drugs; the PAG, PB and DR contained fewer c-fos+ neurons in both drug-treated groups.

4. Conclusions

In this work, we evaluated the effects of pretreatment with ACH-000029 or prazosin on brain c-fos activation following SPS exposure in mice. The study contributes to the literature in three important ways. First, to our knowledge, it provides for the first time a comprehensive brain map of c-fos based activation in the SPS model, revealing neural circuits triggered by the traumatic experience. Second, it describes areas that are regulated by ACH-0000029 or prazosin, pointing to specific 5-HT- versus α1-adrenergic-mediated actions in brain structures implicated in PTSD. Third, it corroborates our previous findings in which ACH-000029 treatment in the early post-SPS period prevented the appearance of PTSD-like symptoms in the SPS model (Azevedo et al., 2020), highlighting its potential use as a pharmacotherapy in the peri-trauma or early post-trauma period to mitigate the stress response that leads to PTSD development.

The SPS protocol is a well-established stress paradigm that has been used to model intense acute stress. Accordingly, some of the brain structures activated by SPS were already associated with the circuitry dysfunctions observed in the rodent brain and in PTSD patients (Fenster et al., 2018); these structures include parts of the medial frontal, dorsal, and lateral cortices, the hippocampal formation, the basal nuclei, the amygdala, the hypothalamus, the midbrain and the hindbrain. Previous studies in which the SPS model was used have shown alterations in c-fos expression in the ventral and dorsal hippocampus, the basolateral amygdala, the infralimbic cortex, the periaqueductal gray and the

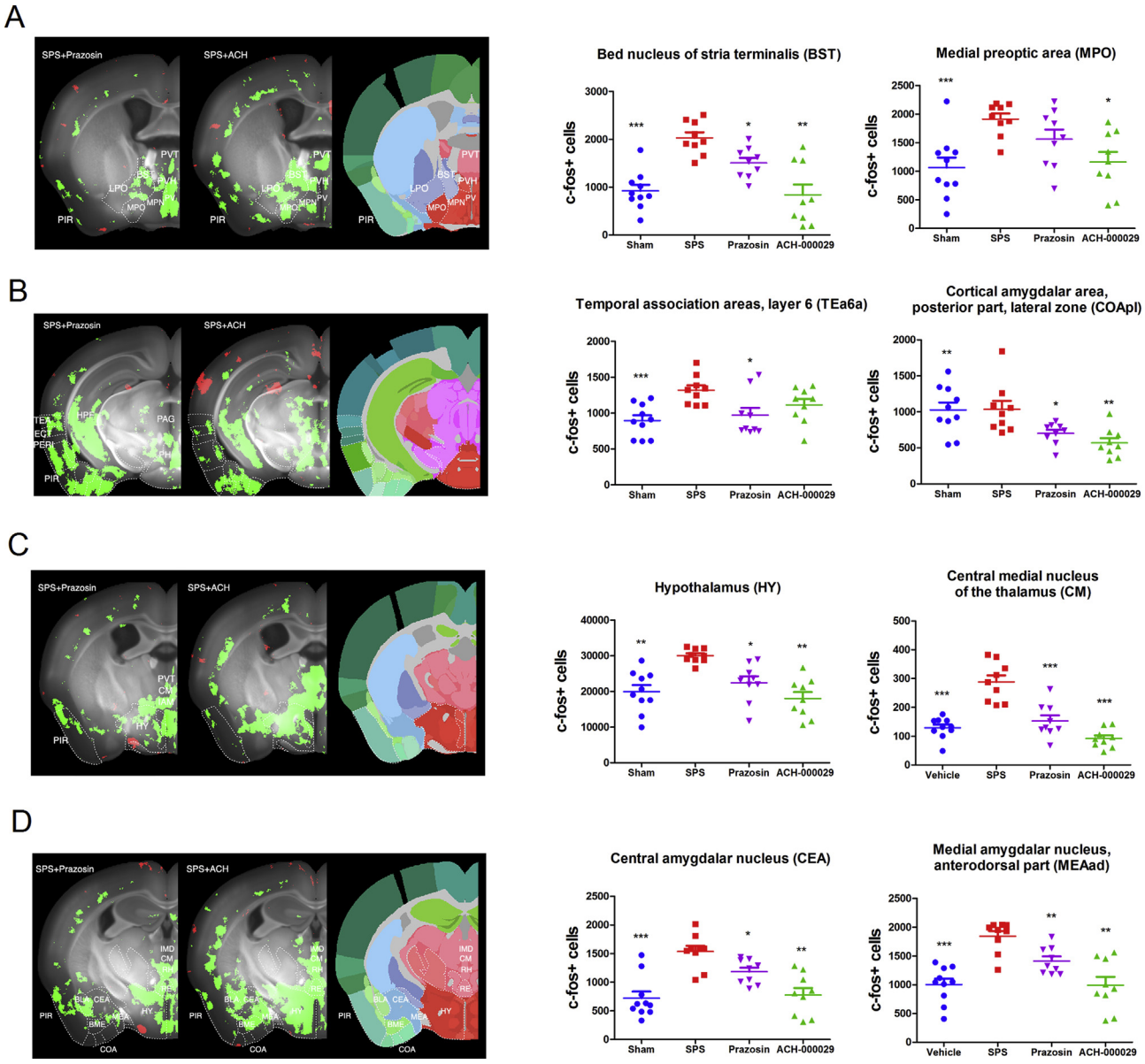

Fig. 5. Anatomical description of brain regions regulated in the drug-pretreated groups compared to the Vehicle-SPS group. The data are reported as bar graph representations (mean + S.E.M.) or anatomical visualizations in which neuronal activation (increase in c-fos + cells counts) or inhibition (decrease in c-fos + cell counts) are visualized, respectively, as red or green signals overlaid on a grayscale image of a mouse brain. (A) The decrease in the number of c-fos + cells in BST and hypothalamic areas, such as the PVH, MPO, and LPO, was higher in the ACH-000029-SPS group (panel SPS + ACH). This was also true for the piriform cortex (PIR) and the paraventricular thalamus (PVT). (B) Inhibition in the hippocampal formation (HPF) and the cortical amygdala (COA) was similar, while inhibition in the PIR, the lateral association cortices (TEA, ECT, PERI) and the periaqueductal gray (PAG) was more pronounced in the ACH-000029-SPS group. (C) Inhibition in the hypothalamus (HY) and the midline thalamic nuclei (PVT, CM, IAM) was more pronounced in the ACH-000029-SPS group. (D) The number of c-fos + cells in the central (CEA) and medial amygdala (MEA) was lower in the ACH-000029-SPS group, while inhibition in the BLA was similar in the two groups. *q < 0.05, **q < 0.01, ***q < 0.001. Statistical comparisons were performed against the Vehicle-SPS group. (For interpretation of the references to color in this figure legend, the reader is referred to the Web version of this article.)

midline thalamic nuclei, regions that are critical to fear extinction and retention and to emotional learning (Knox et al., 2016; Della Valle et al., 2019).

The main limitation of this study is that the SPS-induced brain activation profile was mapped at a short latency after the SPS protocol using a single marker of neuronal activity (c-fos). Therefore, further studies should be performed using other time points and other neuronal activation markers to describe the temporal dynamics of neurotransmitters and differentiate the activation of excitatory and inhibitory cells that occur after acute intense stress.

The SPS-induced effects in several regions previously implicated in the stress response were partially blocked by prazosin pretreatment but fully blocked by ACH-000029 pretreatment. Prazosin was shown to prevent brain c-fos expression in rodents when used prior to stress challenges such as immobilization stress (Stone and Zhang, 1995) and reinstatement of alcohol-seeking behavior (Funk et al., 2016). However, pretreatment with prazosin did not fully inhibit corticotropin-releasing hormone expression after acute stress (Kiss and Aguilera, 2000), nor did it attenuate c-fos expression in the paraventricular nucleus or corticosterone secretion after restraint stress (Williams and Morilak, 1997). These results reinforce the evidence that α1-adrenergic signaling is necessary but not sufficient to elicit an acute stress response in the brain.

ACH-000029 entirely prevented the SPS-driven c-fos activation in

areas essential to the stress-anxiety response, such as the bed nuclei of the stria terminalis, the central and medial amygdala, the pallidum, the paraventricular hypothalamus, the cuneiform nucleus, the periaqueductal gray and thalamic structures including the mediodorsal, intermediodorsal and central medial nuclei. These results collectively indicate that dual regulation of 5-HT and α1-adrenergic-mediated neurotransmission is essential to block stress-induced responses in the brain. The lack of significant differences between c-fos+ cell counts from cortical sensory areas in the ACH-000029-SPS and Vehicle-SPS groups suggests that ACH-000029 specifically blocked the stress response rather than affected sensory areas in the brain. The inhibition of the stress circuitry during SPS may attenuate the long-term effects of the trauma, by controlling the stress experience and the resulting brain activation induced by the SPS protocol.

CRediT authorship contribution statement

Hatylas Azevedo: Conceptualization, Methodology, Formal analysis, Writing - original draft. **Marcos Ferreira:** Methodology, Visualization, Formal analysis, Writing - review & editing. **Alessandra Mascarello:** Project administration, Formal analysis, Writing - review & editing. **Pavel Osten:** Methodology, Investigation, Data curation. **Cristiano Ruch Werneck Guimarães:** Conceptualization, Supervision, Writing - review & editing.

Declaration of competing interest

HA, MF, AM and CRWG are employed by Ache Laboratórios Farmacêuticos. PO is the co-founder of Certerra Inc.

Acknowledgements

We thank the contribution of Mihail Bota in the anatomical description of the c-fos data.

Appendix A. Supplementary data

Supplementary data to this article can be found online at https://doi.org/10.1016/j.ynstr.2020.100226.

References

Adhikari, A., 2014. Distributed circuits underlying anxiety. Front. Behav. Neurosci. 8, 112.
American Psychiatric Association, 2013. Diagnostic and Statistical Manual of Mental Disorder, fifth ed. Publisher, Washington, DC.
Aspesi, D., Pinna, G., 2019. Animal models of post-traumatic stress disorder and novel treatment targets. Behav. Pharmacol. 30, 130–150.
Azevedo, H., Ferreira, M., Costa, R.W., Russo, V., Russo, E., Mascarello, A., Guimaraes, C.R.W., 2019. Preclinical characterization of ACH-000029, a novel anxiolytic compound acting on serotonergic and alpha-adrenergic receptors. Prog. Neuropsychopharmacol. Biol. Psychiatr. 95, 109707.
Azevedo, H., Ferreira, M., Mascarello, A., Osten, P., Werneck Guimarães, C.R., 2020. The serotonergic and alpha-1 adrenergic receptor modulator ACH-000029 ameliorates anxiety-like behavior in a post-traumatic stress disorder model. Neuropharmacology 164, 107912.
Benjamini, Y., Hochberg, Y., 1995. Controlling the false discovery rate: a practical and powerful approach to multiple testing. J. Roy. Stat. Soc. B 57 (1), 289–300.
Bernardy, N.C., Friedman, M.J., 2015. Psychopharmacological strategies in the management of posttraumatic stress disorder (PTSD): what have we learned? Curr. Psychiatr. Rep. 17, 564.
Bisler, S., Schleicher, A., Gass, P., Stehle, J.H., Zilles, K., Staiger, J.F., 2002. Expression of c-Fos, ICER, Krox-24 and JunB in the whisker-to-barrel pathway of rats: time course of induction upon whisker stimulation by tactile exploration of an enriched environment. J. Chem. Neuroanat. 23 (3), 187–198.
Borghans, B., Homberg, J.R., 2015. Animal models for posttraumatic stress disorder: an overview of what is used in research. World J. Psychiatr. 5 (4), 387–396.
Bryant, R., 2018. Treatment of Acute Stress Disorder in Adults. UpToDate Retrieved from. https://www.uptodate.com/contents/treatment-of-acute-stress-disorder-in-adults.
Burbiel, J.C., 2015. Primary prevention of posttraumatic stress disorder: drugs and implications. Mil. Med. Res. 2, 24.
ClinicalTrialsgov [Internet] Bethesda (MD) National library of medicine (US). Identifier NCT03045016, efficacy of prazosin in preventing post-traumatic stress disorder (PRAZOSTRESS). Available from: https://clinicaltrials.gov/ct2/show/NCT03045016.
Comoli, E., Ribeiro-Barbosa, E.R., Canteras, N.S., 2003. Predatory hunting and exposure to a live predator induce opposite patterns of Fos immunoreactivity in the PAG. Behav. Brain Res. 138 (1), 17–28.
De Bartolomeis, A., Buonaguro, E.F., Latte, G., Rossi, R., Marmo, F., Iasevoli, F., Tomasetti, C., 2017. Immediate-early genes modulation by antipsychotics: translational implications for a putative gateway to drug-induced long-term brain changes. Front. Behav. Neurosci. 11, 240.
De Berardis, D., Marini, S., Serroni, N., Iasevoli, F., Tomasetti, C., de Bartolomeis, A., Mazza, M., Tempesta, D., Valchera, A., Fornaro, M., Pompili, M., Sepede, G., Vellante, F., Orsolini, L., Martinotti, G., Di Giannantonio, M., 2015. Targeting the noradrenergic system in posttraumatic stress disorder: a systematic review and meta-analysis of prazosin trials. Curr. Drug Targets 16 (10), 1094–1106.
Della Valle, R., Mohammadmirzaei, N., Knox, D., 2019. Single prolonged stress alters neural activation in the periacqueductal gray and midline thalamic nuclei during emotional learning and memory. Learn. Mem. 26 (10), 1–9.
Deslauriers, J., Toth, M., Der-Avakian, A., Risbrough, V.B., 2018. Current status of animal models of posttraumatic stress disorder: behavioral and biological phenotypes, and future challenges in improving translation. Biol. Psychiatr. 83 (10), 895–907.
Fanselow, M.S., Dong, H.W., 2010. Are the dorsal and ventral hippocampus functionally distinct structures? Neuron 65 (1), 7–19.
Fenster, R.J., Lebois, L.A.M., Ressler, K.J., Suh, J., 2018. Brain circuit dysfunction in post-traumatic stress disorder: from mouse to man. Nat. Rev. Neurosci. 19 (9), 535–551.
Flandreau, E.I., Toth, M., 2018. Animal models of PTSD: a critical review. Curr. Top. Behav. Neurosci. 38, 47–68.
Funk, D., Coen, K., Tamadon, S., Li, Z., Loughlin, A., Lê, A.D., 2016. Effects of prazosin and doxazosin on yohimbine-induced reinstatement of alcohol seeking in rats. Psychopharmacology (Berl). 233 (11), 2197–2207.
Gallo, F.T., Katche, C., Morici, J.F., Medina, J.H., Weisstaub, N.V., 2018. Immediate early genes, memory and psychiatric disorders: focus on c-fos, Egr1 and arc. Front. Behav. Neurosci. 12, 79.
Girotti, M., Pace, T.W., Gaylord, R.I., Rubin, B.A., Herman, J.P., Spencer, R.L., 2006. Habituation to repeated restraint stress is associated with lack of stress-induced c-fos expression in primary sensory processing areas of the rat brain. Neuroscience 138 (4), 1067–1081.
Green, B., 2014. Prazosin in the treatment of PTSD. J. Psychiatr. Pract. 20 (4), 253–259.
Herman, J.P., McKlveen, J.M., Ghosal, S., Kopp, B., Wulsin, A., Makinson, R., Scheimann, J., Myers, B., 2016. Regulation of the hypothalamic-pituitary-adrenocortical stress response. Comp. Physiol. 6 (2), 603–621.
Herman, J.P., Tasker, J.G., 2016. Paraventricular hypothalamic mechanisms of chronic stress adaptation. Front. Endocrinol. 7, 137.
Hendrickson, R.C., Raskind, M.A., 2016. Noradrenergic dysregulation in the pathophysiology of PTSD. Exp. Neurol. 284 (Pt B), 181–195.
Hoffman, G.E., Smith, M.S., Verbalis, J.G., 1993. c-Fos and related immediate early gene products as markers of activity in neuroendocrine systems. Front. Neuroendocrinol. 14 (3), 173–213.
Khachatryan, D., Groll, D., Booij, L., Sepehry, A.A., Schütz, C.G., 2016. Prazosin for treating sleep disturbances in adults with posttraumatic stress disorder: a systematic review and meta-analysis of randomized controlled trials. Gen. Hosp. Psychiatr. 39, 46–52.
Kim, Y., Venkataraju, K.U., Pradhan, K., Mende, C., Taranda, J., Turaga, S.C., Arganda-Carreras, I., Ng, L., Hawrylycz, M.J., Rockland, K.S., Seung, H.S., Osten, P., 2015. Mapping social behavior-induced brain activation at cellular resolution in the mouse. Cell Rep. 10 (2), 292–305.
Kim, Y., Perova, Z., Mirrione, M.M., Pradhan, K., Henn, F.A., Shea, S., Osten, P., Li, B., 2016. Whole-brain mapping of neuronal activity in the learned helplessness model of depression. Front. Neural Circ. 10, 3.
Kiss, A., Aguilera, G., 2000. Role of alpha-1-adrenergic receptors in the regulation of corticotropin-releasing hormone mRNA in the paraventricular nucleus of the hypothalamus during stress. Cell. Mol. Neurobiol. 20 (6), 683–694.
Knauber, J., Müller, W.E., 2000. Subchronic treatment with prazosin improves passive avoidance learning in aged mice: possible relationships to alpha1-receptor up-regulation. J. Neural. Transm. 107 (12), 1413–1426.
Knox, D., Stanfield, B.R., Staib, J.M., David, N.P., Keller, S.M., DePietro, T., 2016. Neural circuits via which single prolonged stress exposure leads to fear extinction retention deficits. Learn. Mem. 23 (12), 689–698.
Korte, S.M., Jaarsma, D., Luiten, P.G., Bohus, B., 1992. Mesencephalic cuneiform nucleus and its ascending and descending projections serve stress-related cardiovascular responses in the rat. J. Auton. Nerv. Syst. 41 (1–2), 157–176.
Krystal, J.H., Neumeister, A., 2009. Noradrenergic and serotonergic mechanisms in the neurobiology of posttraumatic stress disorder and resilience. Brain Res. 1293, 13–23.
Lazaridis, I., Tzortzi, O., Weglage, M., Märtin, A., Xuan, Y., Parent, M., Johansson, Y., Fuzik, J., Fürth, D., Fenno, L.E., Ramakrishnan, C., Silberberg, G., Deisseroth, K., Carlén, M., Meletis, K., 2019. A hypothalamus-habenula circuit controls aversion. Mol. Psychiatr. 24 (9), 1351–1368.
Lebow, M.A., Chen, A., 2016. Overshadowed by the amygdala: the bed nucleus of the stria terminalis emerges as key to psychiatric disorders. Mol. Psychiatr. 21 (4), 450–463.
Liberzon, I., López, J.F., Flagel, S.B., Vázquez, D.M., Young, E.A., 1999. Differential regulation of hippocampal glucocorticoid receptors mRNA and fast feedback: relevance to post-traumatic stress disorder. J. Neuroendocrinol. 11 (1), 11–17.
Lin, X., Itoga, C.A., Taha, S., Li, M.H., Chen, R., Sami, K., Berton, F., Francesconi, W., Xu, X., 2018. c-Fos mapping of brain regions activated by multi-modal and electric foot shock stress. Neurobiol. Stress 8, 92–102.
Linares, I.M.P., Corchs, F.D.F., Chagas, M.H.N., Zuardi, A.W., Martin-Santos, R., Crippa,

J.A.S., 2017. Early interventions for the prevention of PTSD in adults: a systematic literature review. Archiv. Clin. Psychiatr. (São Paulo) 44 (1), 23–29.
Lisieski, M.J., Eagle, A.L., Conti, A.C., Liberzon, I., Perrine, S.A., 2018. Single-prolonged stress: a review of two decades of progress in a rodent model of post-traumatic stress disorder. Front. Psychiatr. 9, 196.
Liu, H., Wang, H.T., Han, F., Shi, Y.X., 2011. Activity of 5-HT1A receptor is involved in neuronal apoptosis of the amygdala in a rat model of post-traumatic stress disorder. Mol. Med. Rep. 4 (2), 291–295.
Luo, F.F., Han, F., Shi, Y.X., 2011. Changes in 5-HT1A receptor in the dorsal raphe nucleus in a rat model of post-traumatic stress disorder. Mol. Med. Rep. 4 (5), 843–847.
Malikowska, N., Ł, Fijałkowski, Nowaczyk, A., Popik, P., Sałat, K., 2017. Antidepressant-like activity of venlafaxine and clonidine in mice exposed to single prolonged stress - a model of post-traumatic stress disorder. Pharmacodynamic and molecular docking studies. Brain Res. 1673, 1–10.
Martinez, M., Calvo-Torrent, A., Herbert, J., 2002. Mapping brain response to social stress in rodents with c-fos expression: a review. Stress 5 (1), 3–13.
Moench, K.M., Breach, M.R., Wellman, C.L., 2019. Chronic stress produces enduring sex- and region-specific alterations in novel stress-induced c-Fos expression. Neurobiol. Stress 10, 100147.
Mutch, J., Knoblich, U., Poggio, T., 2010. CNS: a GPU-¬-based Framework for Simulating Cortically-Organized Networks. Massachusetts Institute of Technology, Cambridge, MA Tech Rep MIT-CSAIL-TR-2010-013/CBCL-286.
Olson, V.G., Rockett, H.R., Reh, R.K., Redila, V.A., Tran, P.M., Venkov, H.A., Defino, M.C., Hague, C., Peskind, E.R., Szot, P., Raskind, M.A., 2011. The role of norepinephrine in differential response to stress in an animal model of posttraumatic stress disorder. Biol. Psychiatr. 70 (5), 441–448.
Osten, P., Margrie, T.W., 2013. Mapping brain circuitry with a light microscope. Nat. Methods 10 (6), 15–23.
Perrine, S.A., Eagle, A.L., George, S.A., Mulo, K., Kohler, R.J., Gerard, J., Harutyunyan, A., Hool, S.M., Susick, L.L., Schneider, B.L., Ghoddoussi, F., Galloway, M.P., Liberzon, I., Conti, A.C., 2016. Severe, multimodal stress exposure induces PTSD-like characteristics in a mouse model of single prolonged stress. Behav. Brain Res. 303, 228–237.
Rajbhandari, A.K., Baldo, B.A., Bakshi, V.P., 2015. Predator stress-induced CRF release causes enduring sensitization of basolateral amygdala norepinephrine systems that promote PTSD-like startle abnormalities. J. Neurosci. 35 (42), 14270–14285.
Renier, N., Adams, E.L., Kirst, C., Wu, Z., Azevedo, R., Kohl, J., Autry, A.E., Kadiri, L., Umadevi Venkataraju, K., Zhou, Y., Wang, V.X., Tang, C.Y., Olsen, O., Dulac, C., Osten, P., Tessier-Lavigne, M., 2016. Mapping of brain activity by automated volume Analysis of immediate early genes. Cell 165 (7), 1789–1802.
Roque, A.P., 2015. Pharmacotherapy as prophylactic treatment of post-traumatic stress disorder: a review of the literature. Issues Ment. Health Nurs. 36 (9), 740–751.
Starke, J.A., Stein, D.J., 2017. Management of treatment-resistant posttraumatic stress disorder. Curr. Treat. Opt. Psychiatr. 4 (4), 387–403.
Souza, R.R., Noble, L.J., McIntyre, C.K., 2017. Using the single prolonged stress model to examine the pathophysiology of PTSD. Front. Pharmacol. 8, 615.
Stone, E.A., Zhang, Y., 1995. Adrenoceptor antagonists block c-los response to stress in the mouse brain. Brain Res. 694, 279–286.
Toledano, D., Tassin, J.P., Gisquet-Verrier, P., 2013. Traumatic stress in rats induces noradrenergic-dependent long-term behavioral sensitization: role of individual differences and similarities with dependence on drugs of abuse. Psychopharmacology (Berl) 230 (3), 465–476.
Vallès, A., Martí, O., Armario, A., 2006. Long-term effects of a single exposure to immobilization: a c-fos mRNA study of the response to the homotypic stressor in the rat brain. J. Neurobiol. 66 (6), 591–602.
VanElzakker, M., Fevurly, R.D., Breindel, T., Spencer, R.L., 2008. Environmental novelty is associated with a selective increase in Fos expression in the output elements of the hippocampal formation and the perirhinal cortex. Learn. Mem. 15 (12), 899–908.
Vertes, R.P., Linley, S.B., Hoover, W.B., 2015. Limbic circuitry of the midline thalamus. Neurosci. Biobehav. Rev. 54, 89–107.
Wang, H.T., Han, F., Shi, Y.X., 2009. Activity of the 5-HT1A receptor is involved in the alteration of glucocorticoid receptor in hippocampus and corticotropin-releasing factor in hypothalamus in SPS rats. Int. J. Mol. Med. 24 (2), 227–231.
Williams, A.M., Morilak, D.A., 1997. Alpha1B adrenoceptors in rat paraventricular nucleus overlap with, but do not mediate, the induction of c-Fos expression by osmotic or restraint stress. Neuroscience 76 (3), 901–913.
Xiang, M., Jiang, Y., Hu, Z., Yang, Y., Du, X., Botchway, B.O., Fang, M., 2019. Serotonin receptors 2A and 1A modulate anxiety-like behavior in post-traumatic stress disordered mice. Am. J. Transl. Res. 11 (4), 2288–2303.